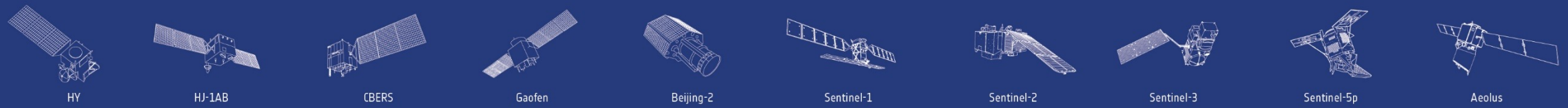

2023 DRAGON 5 SYMPOSIUM

3rd YEAR RESULTS REPORTING

11-15 SEPTEMBER 2023

PROJECT ID. 59318

ALL-WEATHER LAND SURFACE TEMPERATURE AT HIGH SPATIAL RESOLUTION: VALIDATION AND APPLICATIONS

THURSDAY, 14/SEPT/2023

ID. 59318

PROJECT TITLE: ALL-WEATHER LAND SURFACE TEMPERATURE AT HIGH SPATIAL RESOLUTION: VALIDATION AND APPLICATIONS

PRINCIPAL INVESTIGATORS: J. ZHOU AND F.-M. GÖTTSCHE

CO-AUTHORS: W. TANG, L. DING, L. PEREZ-PLANELLS, J. MA, J. MARTINS, Y. MENG AND W. ZHANG

PRESENTED BY: J. MA

- **Objectives:** The main objective is to inter-compare and validate the two new LST products, which provide (nearly) gap-free all-weather LST at high spatial resolution. The two all-weather LST products utilise different retrieval approaches, namely the method by
  - Zhang et al. (2019): temporal component decomposition and merging of TIR LST with passive microwave (PMW) LST.
  - Martins et al. (2019): merging of clear-sky MSG/SEVIRI LST with LST generated by a Soil-Vegetation-Atmosphere (SVAT) model under cloudy conditions.
- **Further objectives:**
  - Generation of long term (global) all-weather LST data set
  - Setting up an LST validation station in China to provide Fiducial Reference Measurements (FRM)
  - Employing all-weather LST data to simulate and study freeze / thaw on the TP

EO Data Delivery

Data access (list all missions and issues if any). NB. in the tables please insert cumulative figures (since July 2020) for no. of scenes of high bit rate data (e.g. S1 100 scenes). If data delivery is low bit rate by ftp, insert “ftp”

ESA /Copernicus Missions	No. Scenes
1. Sentinel-3 SLSTR	
2. MSG SEVIRI	
3.	
4.	
5.	
6.	
Total:	
Issues:	

ESA Third Party Missions	No. Scenes
1. Terra/Aqua MODIS	500+
2.	
3.	
4.	
5.	
6.	
Total:	500+
Issues:	

Chinese EO data	No. Scenes
1. FY-3B MWR	500+
2. FY-4A	500+
3. FY-2 LST	500+
4.	
5.	
6.	
Total:	1500+
Issues:	

European Young scientists contributions in Dragon 5

Name	Institution	Poster title	Contribution including period of research
Lluís Pérez-Planells	Karlsruhe Institute of Technology	Validation of Two All-weather Land Surface Temperature Products over a Long Rainy Season at the Gravel Plains of Gobabeb, Namibia	All-weather LST validation

Chinese Young scientists contributions in Dragon 5

Name	Institution	Poster title	Contribution including period of research
Wenbin Tang	University of Electronic Science and Technology of China	-	All-weather LST generation
Lirong Ding	University of Electronic Science and Technology of China	-	All-weather LST generation
Yizhen Meng	University of Electronic Science and Technology of China	-	All-weather LST validation
Jin Ma	University of Electronic Science and Technology of China	Ground Station Spatial Representativeness In Satellite-retrieved Land Surface Temperature (LST) Validation	All-weather LST validation

Outlook for the progress of Project 59318

I. ALL-WEATHER LST FROM UESTC, CHINA

II. LSA SAF (IPMA) ALL-SKY LST

III. VALIDATION AGAINST IN-SITU LST

IV. SPATIAL REPRESENTATION OF GROUND STATIONS IN LST VALIDATION

V. APPLICATION

Outlook for the progress of Project 59318

I. ALL-WEATHER LST FROM UESTC, CHINA

II. LSA SAF (IPMA) ALL-SKY LST

III. VALIDATION AGAINST IN-SITU LST

IV. SPATIAL REPRESENTATION OF GROUND STATIONS IN LST VALIDATION

V. APPLICATION

I. All-weather LST from UESTC, China ——TRIMS LST (2000-2021) for China

Importance to China and neighboring regions

- Since LST is highly sensitive to land cover change, heat waves, droughts, and vegetation information, making it an important indicator of global climate change, it is important to investigate the spatial and temporal variations of LST for these areas. This requires a long-term, high-quality, and spatio-temporally continuous LST dataset.

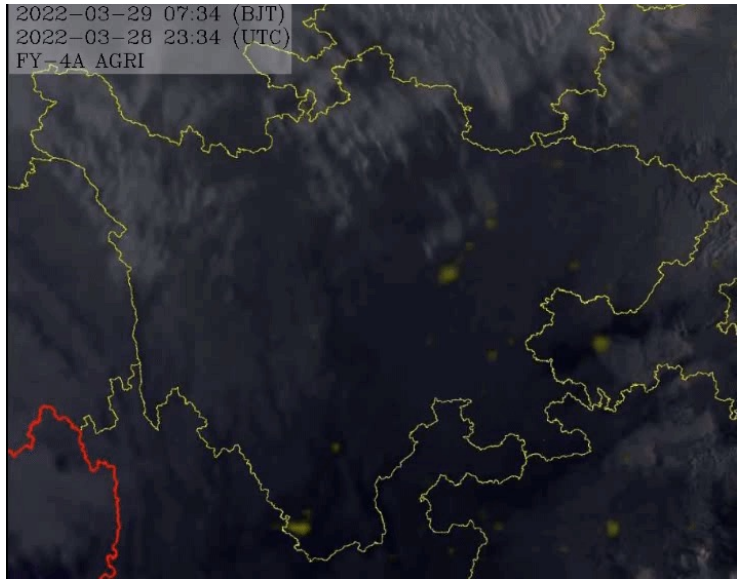

Cloud cover from FY-4A (Sichuan)

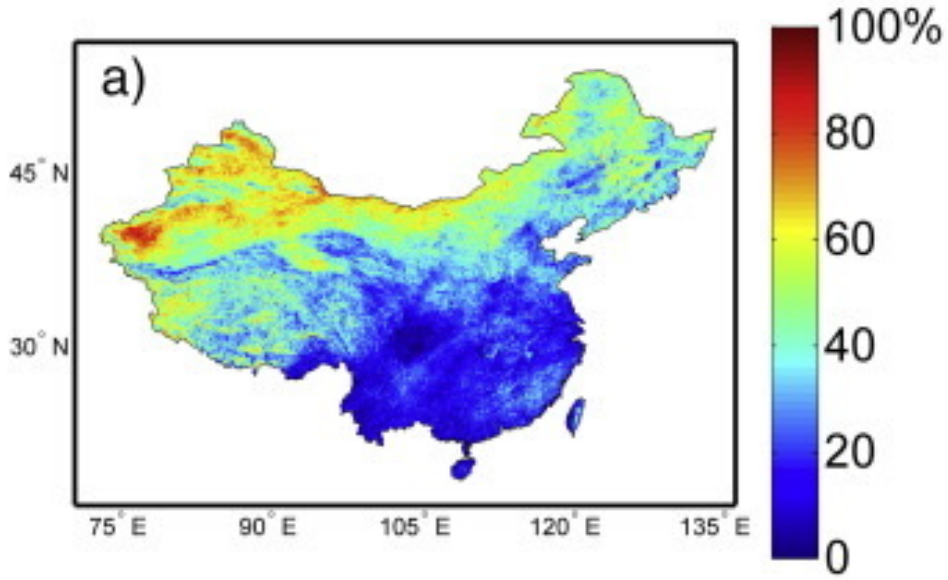

Proportion of pixels in the clear sky in July 2009 (Duan et al., 2017)

I. All-weather LST from UESTC, China ——TRIMS LST (2000-2021) for China

Method

- TRIMS LST is generated through the E-RTM method, consisting of three modules depicted.
- Module I runs the original RTM method to merge MOD11A1 (MYD11A1) and GLDAS LST, producing daily all-weather LST at the Terra (Aqua) satellite overpass time from DOY 55 of 2000 (DOY 185 of 2002) to DOY 365 of 2022.
- Module II employs a Random-Forest based Spatio-Temporal Merging (RFSTM) approach to extend the beginning date of the MOD11A1 LST based all-weather LST to January 1, 2000.
- Finally, Module III utilizes a Time-Sequential LST based Reconstruction (TSETR) approach to extend the beginning date of the MYD11A1 LST based all-weather LST to January 1.

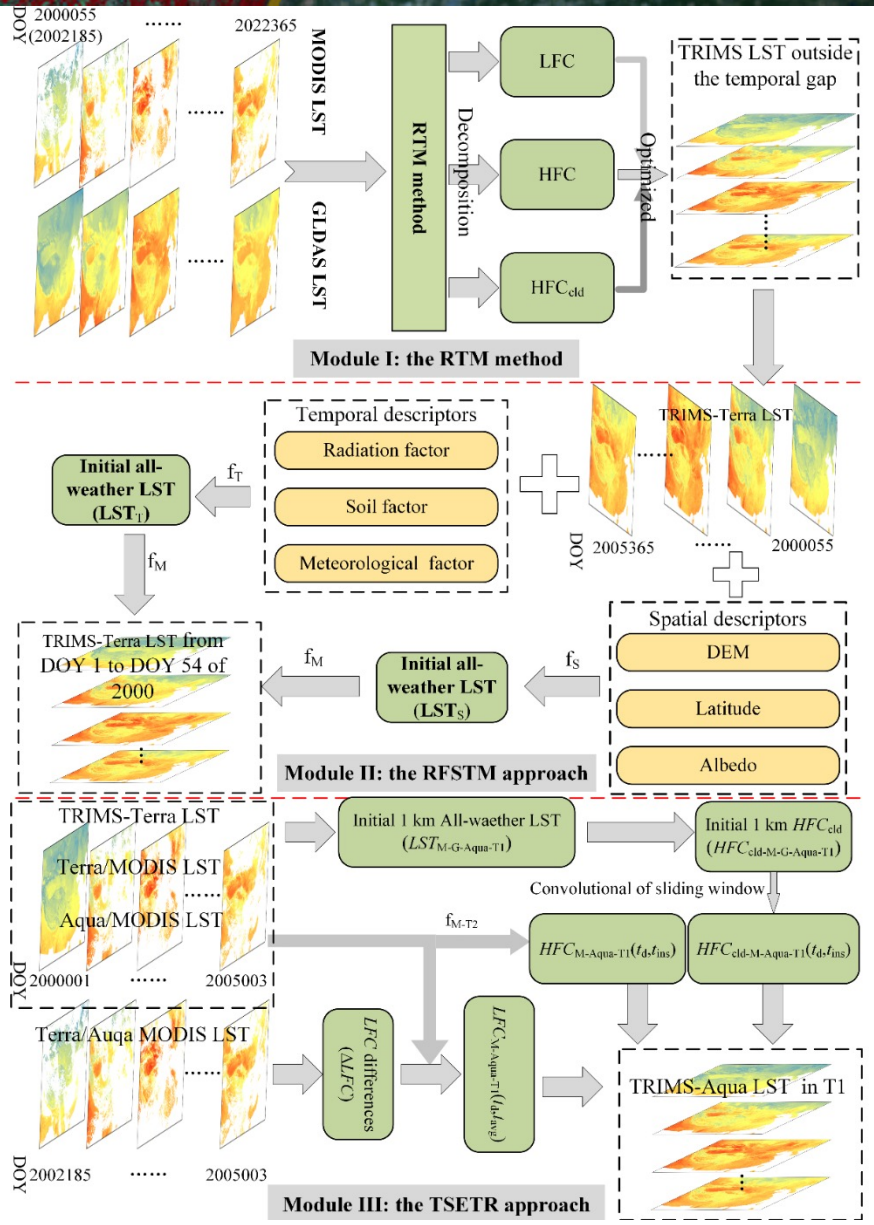

Tang, W., Zhou, J., Ma, J., Wang, Z., Ding, L., Zhang, X., and Zhang, X.: TRIMS LST: **A daily 1-km all-weather land surface temperature dataset for the Chinese landmass and surrounding areas (2000–2021)**, Earth Syst. Sci. Data Discuss. [preprint], https://doi.org/10.5194/essd-2023-27, in review, 2023.

➢ Comparison of the TRIMS LST with reanalysis data

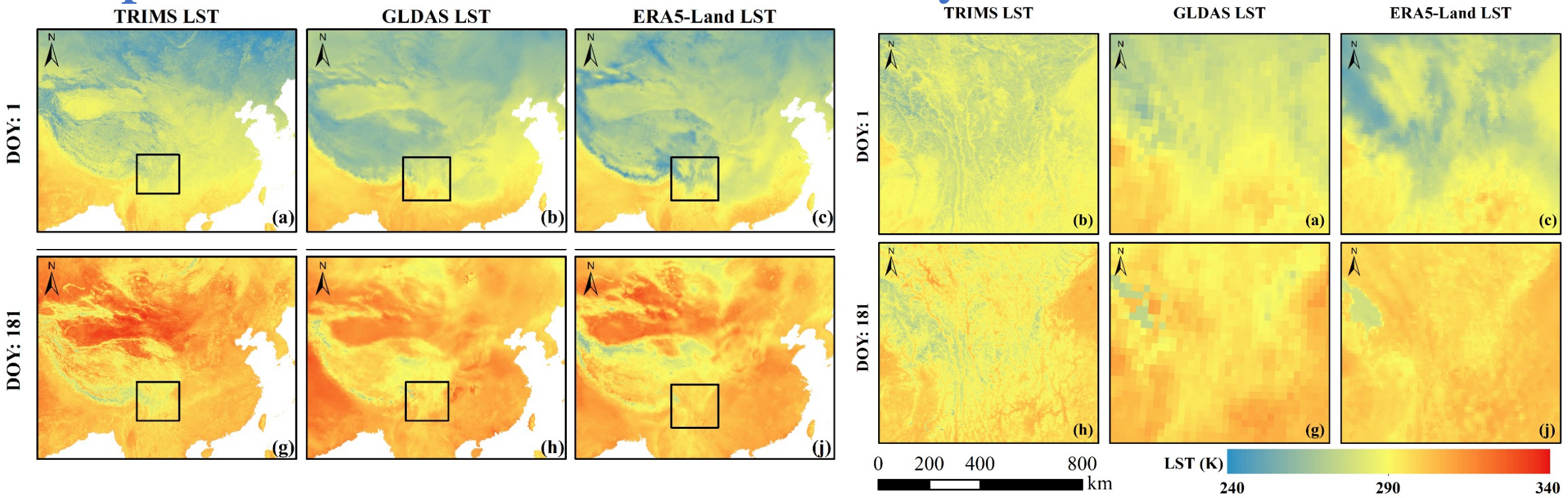

Compared with the GLDAS LST and the ERA5-Land LST, the TRIMS LST offers more spatial details because of its much higher spatial resolution.

➢ Comparison of the TRIMS LST with satellite TIR LST products

- Compared with AATSR, the overall MBD/STD values of TRIMS were 0.37 K/1.55 K and -0.44 K/1.22 K for daytime and nighttime, respectively.
- the daily daytime MBD and STD were mainly concentrated in the ranges of 0 K–0.60 K and 1.05 K–1.15 K, respectively; the daily nighttime MBD and STD were mainly concentrated in the ranges of -0.40 K to 1.0 K and 0.75 K to 1.15 K, respectively.

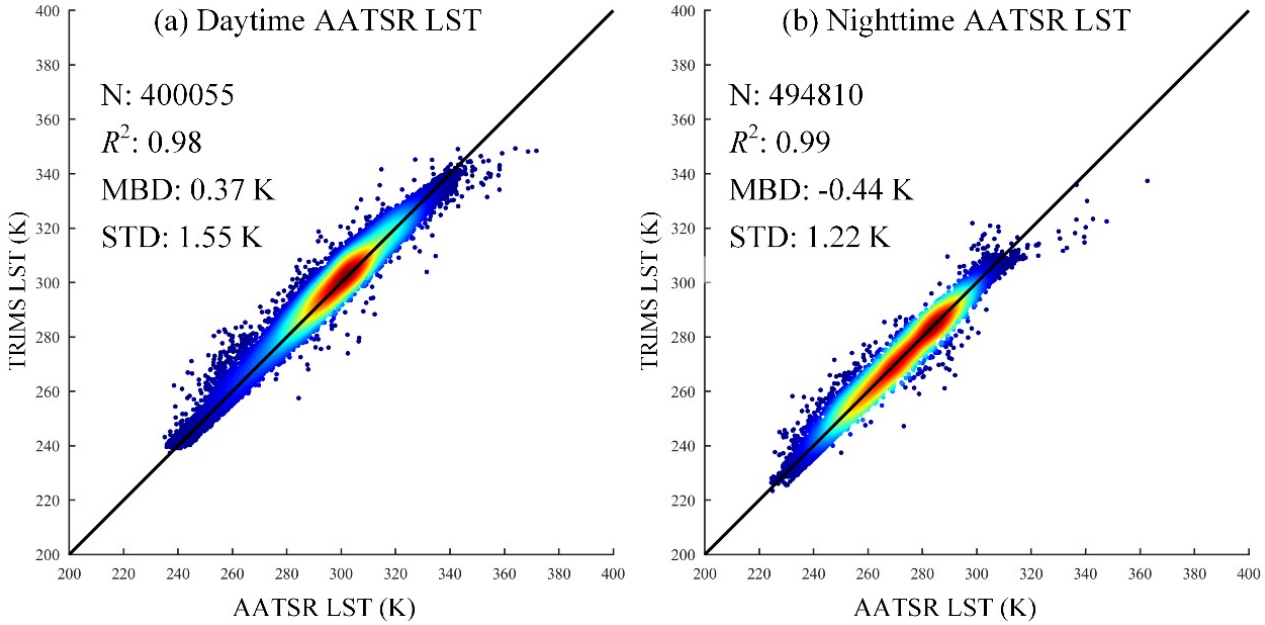

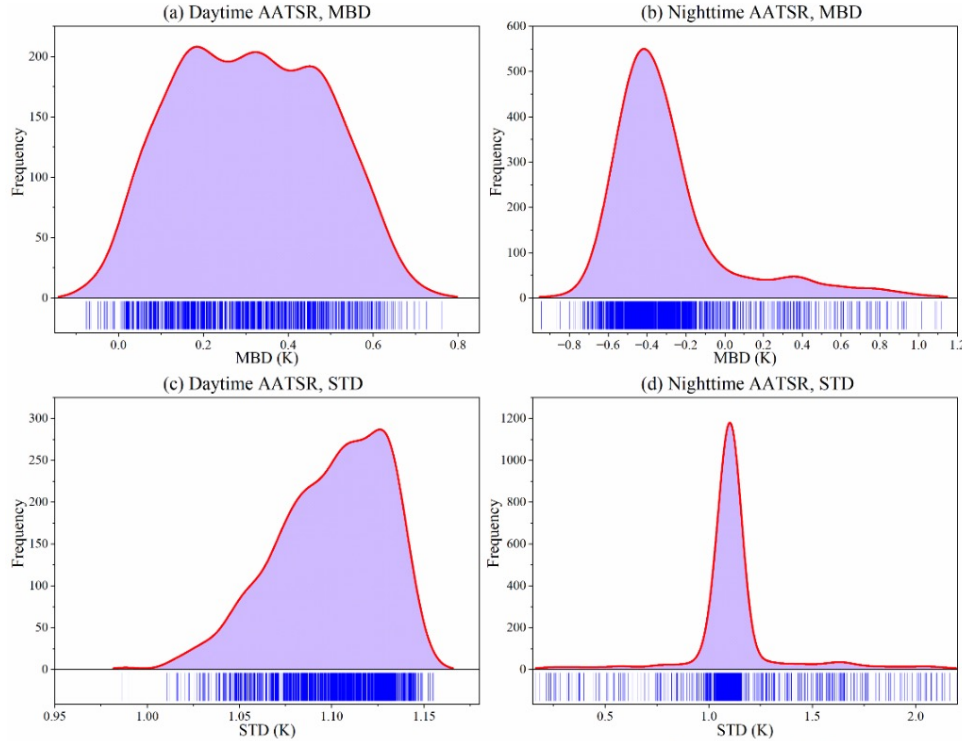

➢ Validation against in-situ LST outside the temporal gap

- Under clear-sky conditions, the TRIMS LST had an accuracy close to that of the MODIS LST
- Under cloudy conditions, the accuracy of TRIMS LST is slightly lower compared to clear-sky conditions, resulting in a 0.35 K increase in the overall RMSE.
- Overall, the validation results indicate that TRIMS LST has good accuracy under cloudy conditions as well as under clear-sky conditions.

R^2, MBE, and RMSE of the daytime validation for different groups.

Group	Land cover type	Condition	Amounts	TRIMS LST			MODIS LST		
				MBE (K)	RMSE (K)	R^2	MBE (K)	RMSE (K)	R^2
I	Grassland	Clear-sky	5370	0.26	2.15	0.95	0.61	2.37	0.95
		Cloudy	6972	0.41	2.18	0.96	–	–	–
II	Desert or barren land	Clear-sky	5930	0.46	2.30	0.98	0.79	2.53	0.98
		Cloudy	5698	0.43	2.26	0.98	–	–	–
III	Cropland	Clear-sky	5738	0.02	2.11	0.97	-0.21	2.52	0.95
		Cloudy	7570	0.04	2.11	0.97	–	–	–
IV	Forest	Clear-sky	3170	0.55	2.46	0.97	0.72	2.38	0.98
		Cloudy	3655	0.68	2.27	0.98	–	–	–

I. All-weather LST from UESTC, China ——Hourly All-weather for TP

Location and background

- TP is selected as the study area(73–106°E and 23–40°N)
- TP has an average elevation of over 4000m
- TP is also one of the most heavily cloud-covered regions in the world
- TP is also known as the “Asian water tower”
- The complex surface characteristics and atmospheric conditions

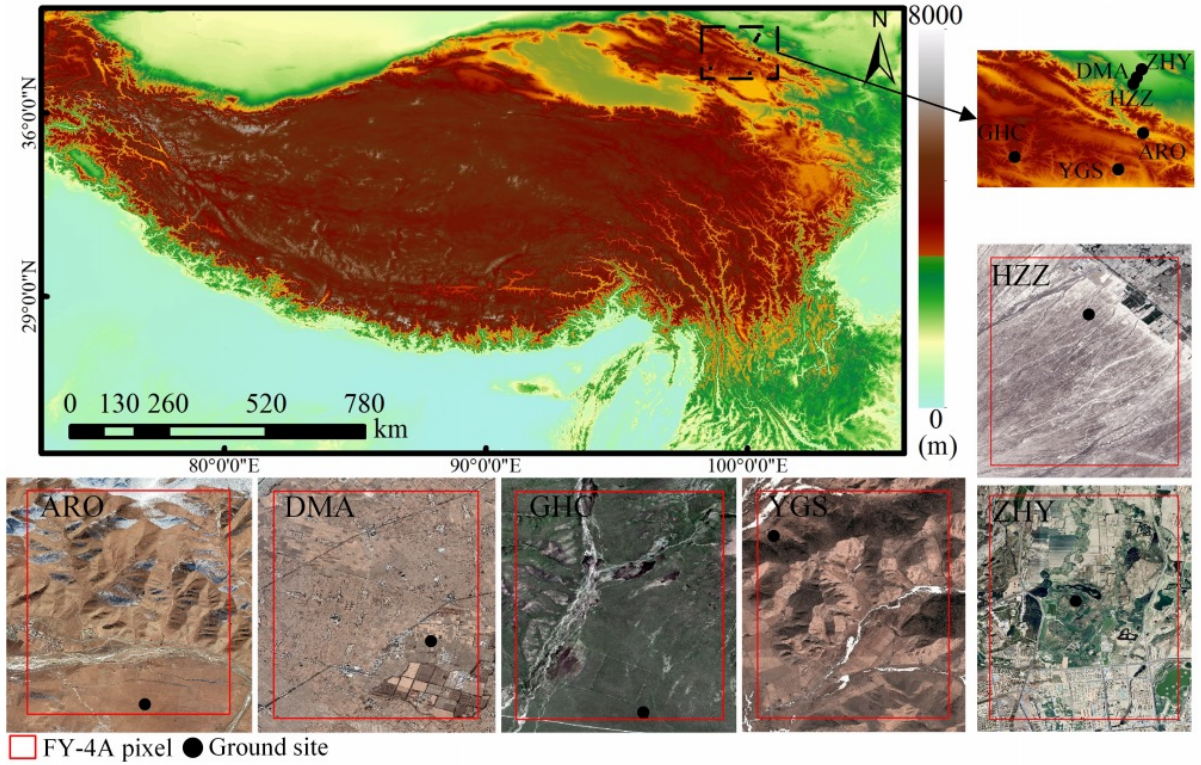

DEM distribution of the study area and land cover conditions of the six selected ground sites.

➢ Method

- The basis of RTG is the LST temporal decomposition theory.
- LST is decomposed into NC and AC.(NC denotes the LST in the ideal state, which is caused by the rotation and revolution of the Earth. AC is a non-regular varying component caused by the weather and surface type)

a) In RTG, we first estimate the initial NC using the ATC model and then fill and optimize the initial NC using the RF and the DTC model.

b) Using the FY-4A AC under clear-sky as a reference, the final AC is obtained after time correction and spatial weighting of the initial AC provided by CLDAS.

Ding, L., Zhou, J., Li, Z.-L., Ma, J., Shi, C., Sun, S., Wang, Z., 2022. **Reconstruction of Hourly All-Weather Land Surface Temperature by Integrating Reanalysis Data and Thermal Infrared Data From Geostationary Satellites (RTG)**. IEEE Trans. Geosci. Remote Sensing 60, 1–17. https://doi.org/10.1109/TGRS.2022.3227074

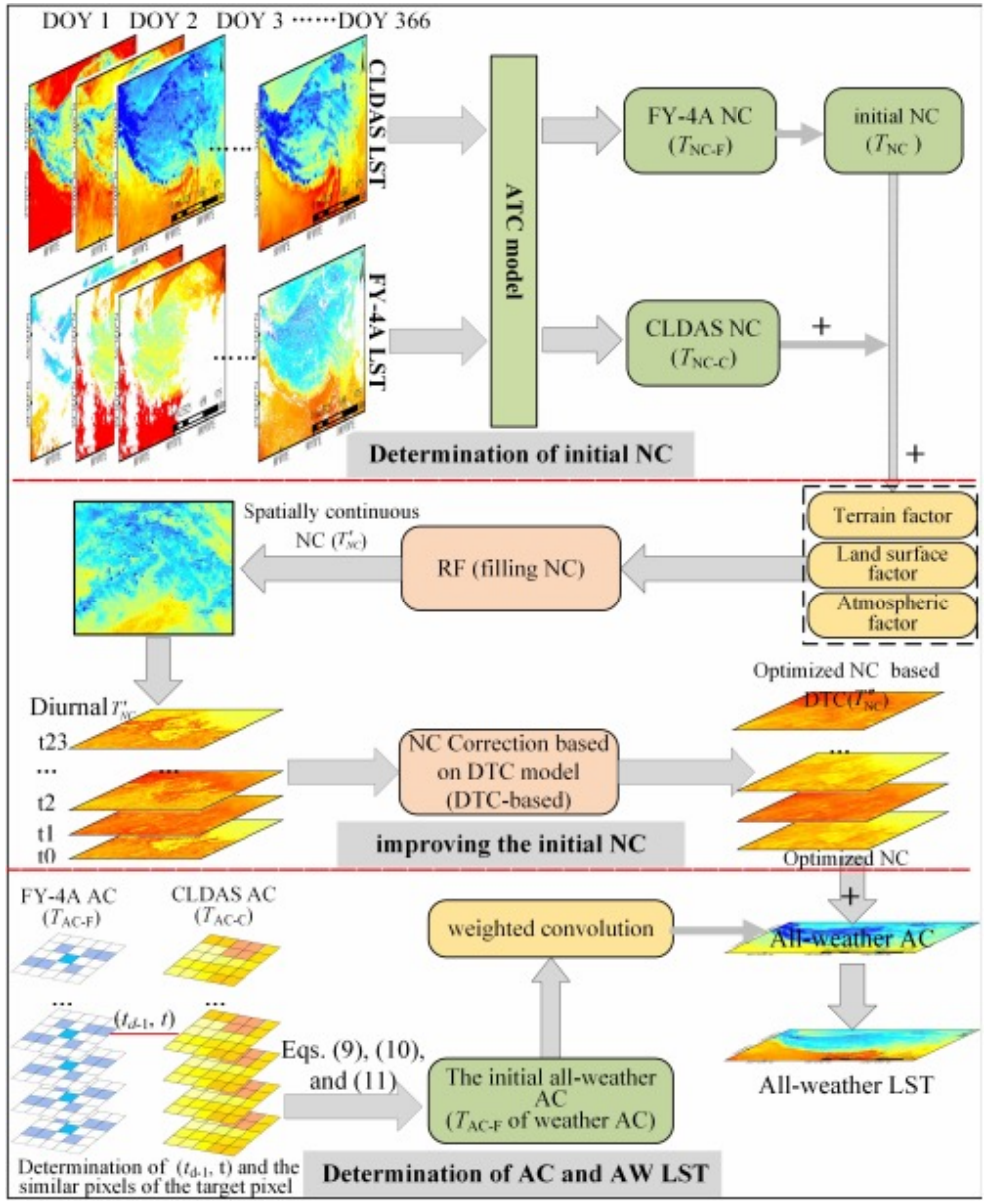

➢ Validation Against the in-situ LST

Site	LST	Clear-sky (Cloudy-sky)				Daytime (Nighttime)				All-weather (All-time)			
		RMSE (K)	MBE (K)	R^2	N	RMSE (K)	MBE (K)	R^2	N	RMSE (K)	MBE (K)	R^2	N
ARO	AW	**2.74 (4.22)**	-0.58 (-2.76)	0.97 (0.93)	3889 (4724)	**3.79 (3.49)**	-1.81 (-1.75)	0.93 (0.94)	3569 (5044)	**3.62**	-1.78	0.95	8613
	CLDAS	5.01 (4.49)	2.03 (-0.27)	0.89 (0.86)	3889 (4274)	5.01 (4.55)	-1.64 (2.81)	0.85 (0.89)	3569 (5044)	4.75	0.97	0.88	8613
DMA	AW	**2.37 (3.73)**	-0.21 (-1.85)	0.97 (0.93)	4004 (4028)	**3.25 (3.02)**	0.09 (-1.84)	0.93 (0.96)	3369 (4663)	**3.12**	-1.03	0.95	8032
	CLDAS	5.40 (4.61)	1.95 (1.14)	0.89 (0.89)	4004 (4028)	6.22 (3.77)	1.62 (1.15)	0.84 (0.90)	3369 (4663)	4.95	1.35	0.89	8032
GHC	AW	**2.73 (4.31)**	0.14 (-1.01)	0.96 (0.90)	1891 (3318)	**4.22 (3.49)**	0.52 (-1.35)	0.87 (0.92)	2114 (3095)	**3.81**	-0.59	0.92	5209
	CLDAS	6.06 (4.68)	1.80 (0.35)	0.85 (0.85)	1891 (3318)	5.84 (3.94)	-1.03 (1.84)	0.78 (0.90)	2114 (3095)	4.81	0.68	0.87	5209
YGS	AW	**3.12 (3.71)**	0.97 (-0.81)	0.94 (0.90)	3868 (4026)	**3.86 (3.08)**	1.56 (-1.01)	0.90 (0.94)	3307 (4587)	**3.43**	0.06	0.93	7894
	CLDAS	6.16 (3.49)	3.75 (-0.66)	0.90 (0.90)	3868 (4026)	3.77 (4.02)	-1.42 (2.17)	0.91 (0.90)	3307 (4587)	4.01	0.67	0.92	7894
HZZ	AW	**2.71 (3.52)**	0.05 (-0.80)	0.97 (0.95)	4487 (4007)	**3.70 (2.62)**	-0.75 (-0.07)	0.95 (0.95)	3533 (4961)	**3.12**	-0.35	0.96	8494
	CLDAS	5.65 (4.74)	2.24 (2.29)	0.89 (0.92)	4487 (4007)	5.07 (5.34)	0.19 (3.74)	0.90 (0.91)	3533 (4961)	5.23	2.27	0.91	8494
ZHY	AW	**4.45 (4.18)**	0.48 (-0.28)	0.92 (0.90)	4837 (3806)	**5.54 (3.18)**	3.74 (-2.42)	0.91 (0.97)	3596 (5047)	**4.33**	0.14	0.92	8643
	CLDAS	6.19 (6.45)	2.30 (3.68)	0.93 (0.93)	4837 (3806)	8.45 (4.01)	5.99 (0.71)	0.94 (0.92)	3596 (5047)	6.26	2.91	0.93	8643

a) The results show that the reconstructed AW LST with RTG has better accuracy (mean RMSE is 3.02 K) for the clear-sky condition than FY-4A and CLDAS LSTs.

b) The AW LST has better accuracy at nighttime than daytime, and a similar case is found for CLDAS LST.

c) The accuracy difference of the reconstructed AW LST by the RTG method between the daytime and nighttime is less than 1 K, indicating that the RTG method has strong applicability in both daytime and nighttime.

➢ Spatial Patterns of AW LST

a) The reconstructed AW LST and FY-4A LST maintain high consistency in magnitude and spatial patterns over the whole TP.

b) RTG can suppress the underestimation of CLDAS LST.

c) There is no obvious “boundary effect” between the clear-sky LST and cloudy-sky LST, indicating that the reconstructed AW LSTs possess good spatial continuity.

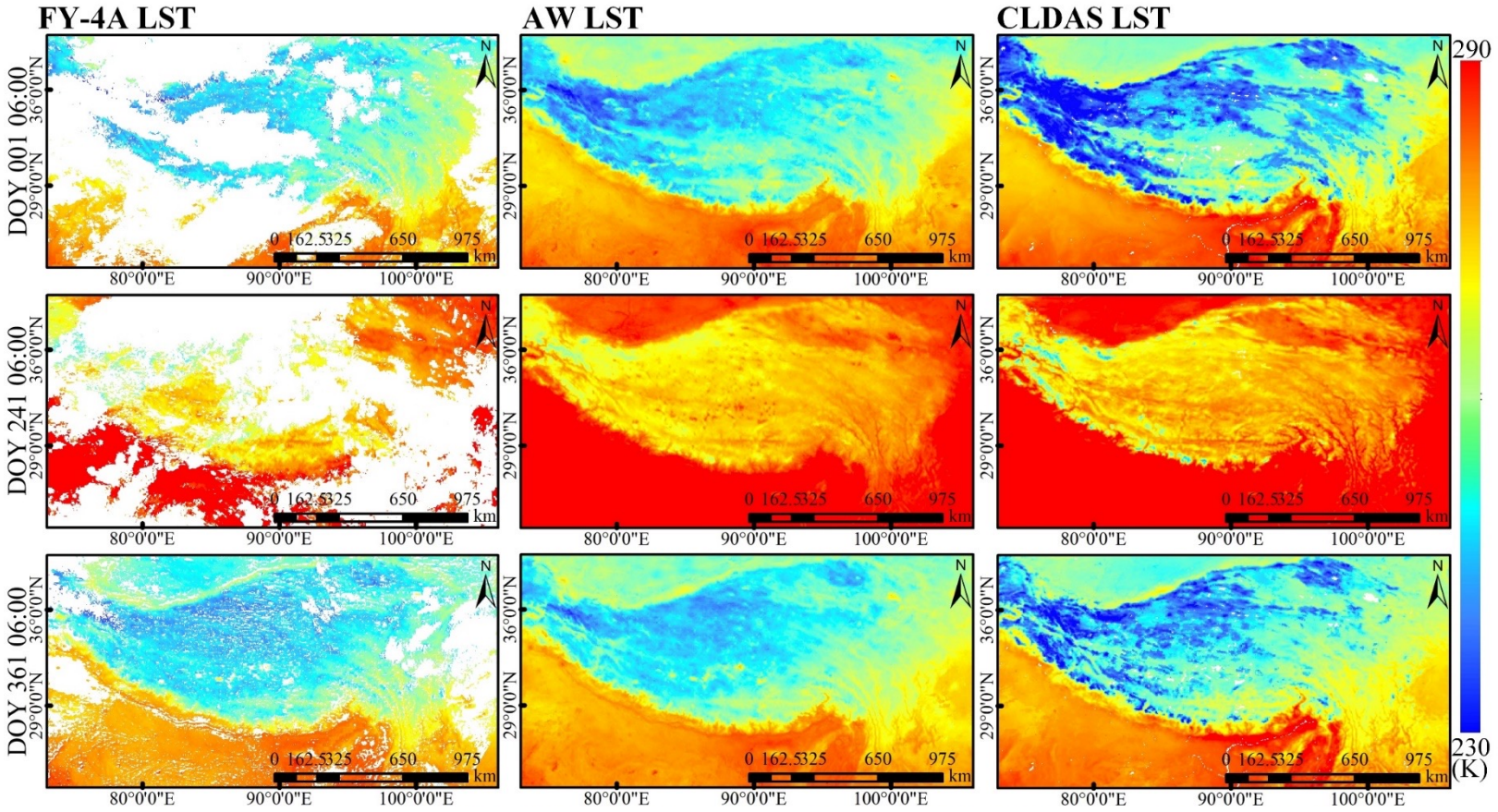

Outlook for the progress of Project 59318

I. ALL-WEATHER LST FROM UESTC, CHINA

II. LSA SAF (IPMA) ALL-SKY LST

III. VALIDATION AGAINST IN-SITU LST

IV. SPATIAL REPRESENTATION OF GROUND STATIONS IN LST VALIDATION

V. APPLICATION

LSA SAF (IPMA) All-Sky LST – will be a CDR!

Clear sky LST

IR retrievals for clear sky (Generalized Split-Windows Algorithm, standard L2 LST for SEVIRI)

Cloudy Sky LST

Skin temperature from a surface energy balance model, forced by LSA-SAF products and ECMWF meteorological data

Inputs:
LSA SAF: $L_{\downarrow}$, $S_{\downarrow}$, Albedo, LAI
ECMWF: Tair, qair, u, v
soil moisture (H-SAF)

Outputs:
H, LE (and evapotranspiration) and SKT

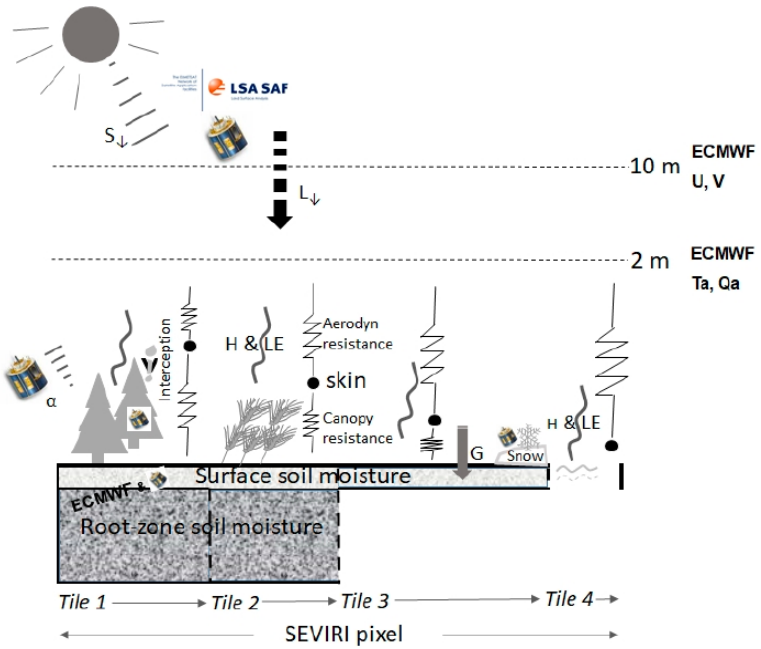

- **Maximizes use of remote sensing data (mostly LSA-SAF)**
- **Scheme based on the H-TESSEL surface model (ECMWF)**
- **Runs every 30 min**
- **Available soon from 2004-onwards**

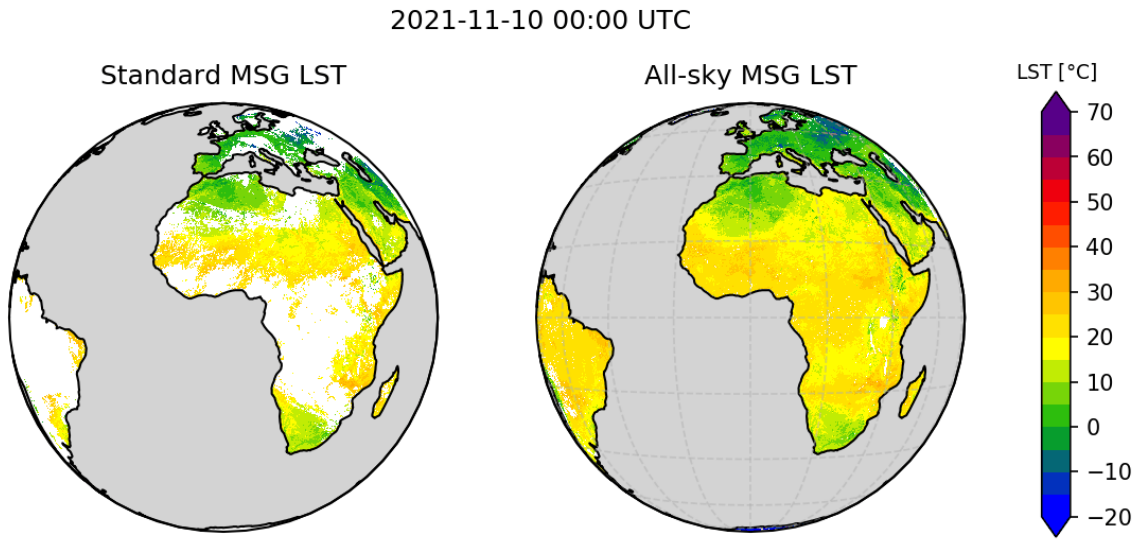

Martins, J., Trigo. I., Ghilain. N., Jimenez. C., Göttsche. F.-M., Ermida, S., Olesen F.-S., Gellens-Meulenberghs, F., Arboleda, A., 2019. An All-Weather Land Surface Temperature Product Based on MSG/SEVIRI Observations. Remote Sensing, doi: 10.3390/rs11243044

LSA SAF (IPMA) All-Sky LST - validation

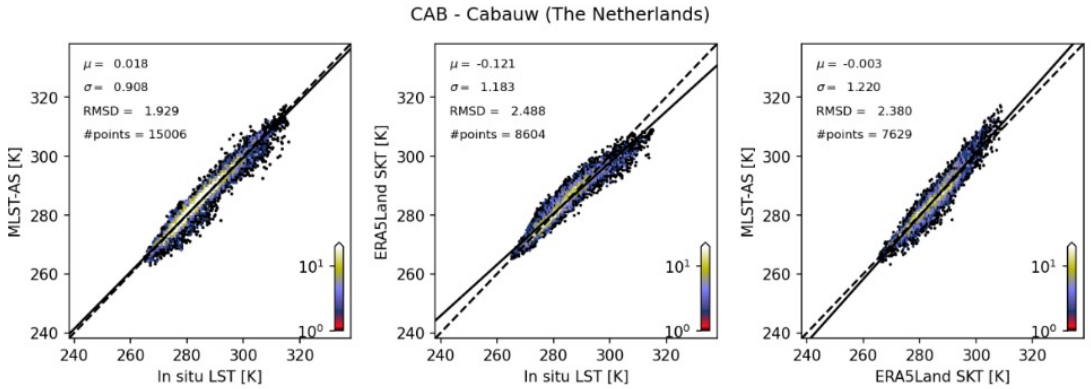

EUMETSAT LSA SAF
LAND SURFACE ANALYSIS

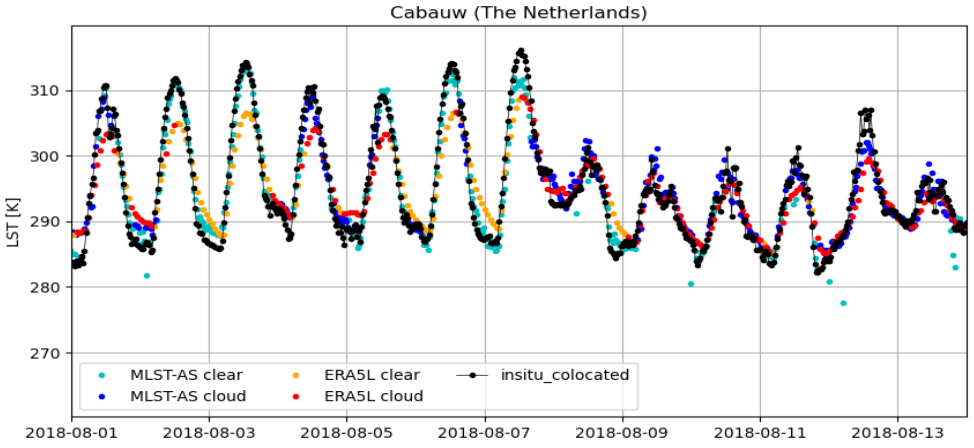

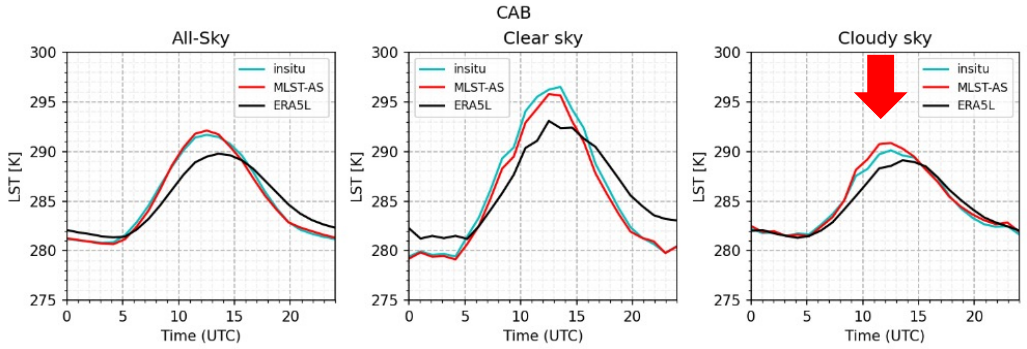

Overall stats for the 33 stations (BSRN + EFDC + KIT)

	MLSTS – *in situ*			ERA5-Land – *in situ*			MLSTS – ERA5-Land		
	All	**Clear**	**Cloudy**	**All**	**Clear**	**Cloudy**	**All**	**Clear**	**Cloudy**
***μ* (K)**	0.0	**-0.2**	**0.2**	0.2	0.1	0.3	-0.2	-0.2	-0.2
***σ* (K)**	1.5	1.4	1.5	1.6	2.1	1.3	1.7	2.1	1.2
RMSD (K)	2.9	2.8	2.8	2.9	3.3	2.6	3.1	3.5	2.4

- **Compares very well with in situ estimates**
- **Statistics for cloudy sky estimates are similar to clear sky**
- **Compares well to ERA5-Land**
- **Some problems in the representation of the diurnal cycle (phase shift, amplitude)**

Outlook for the progress of Project 59318

I. ALL-WEATHER LST FROM UESTC, CHINA

II. LSA SAF (IPMA) ALL-SKY LST

III. VALIDATION AGAINST IN-SITU LST

IV. SPATIAL REPRESENTATION OF GROUND STATIONS IN LST VALIDATION

V. APPLICATION

Investigation and Validation of TRIMS LST and MLST-AS

- Comparison and validation can benefit users in choosing products according to their needs and also help producers improve the corresponding algorithm.
- To facilitate users and producers in understanding the differences between the two all-weather LST generation methods and discuss the global accuracy of TRIMS LST, two all-weather LST products, namely the MLST-AS and TRIMS LST, are selected and validated against *in-situ* measurements from three land sites (i.e., Evora, Gobabeb, and KIT-Forest) and one lake water site (i.e., Lake Constance).
- Due to the inaccurate model representation of the processes involved in the surface EB over water , MLST-AS pixels classified as inland water are routinely masked out and the validation over Lake Constance is limited to TRIMS LST.

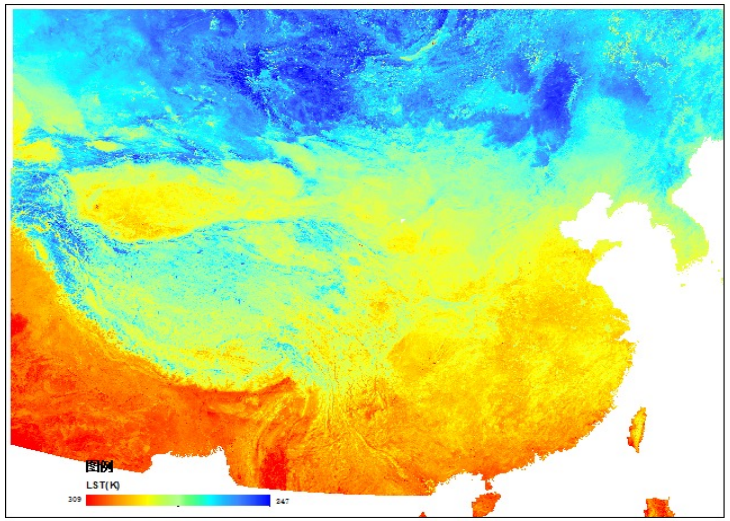

TRIMS LST

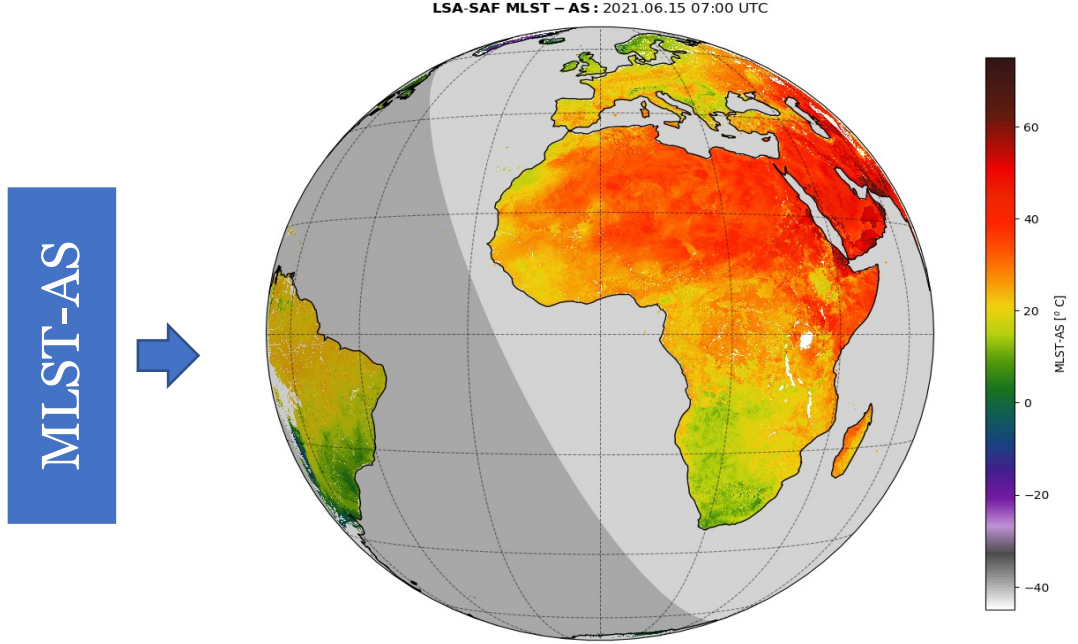

MLST-AS

Investigation and Validation of TRIMS LST and MLST-AS

In-situ measurements are required to validate the performance of the all-weather LST products and gain more information about their quality. We obtain *in-situ* measurements from four ground sites within Europe and Africa, i.e., Evora, Gobabeb, KIT-Forest, and Lake Constance.

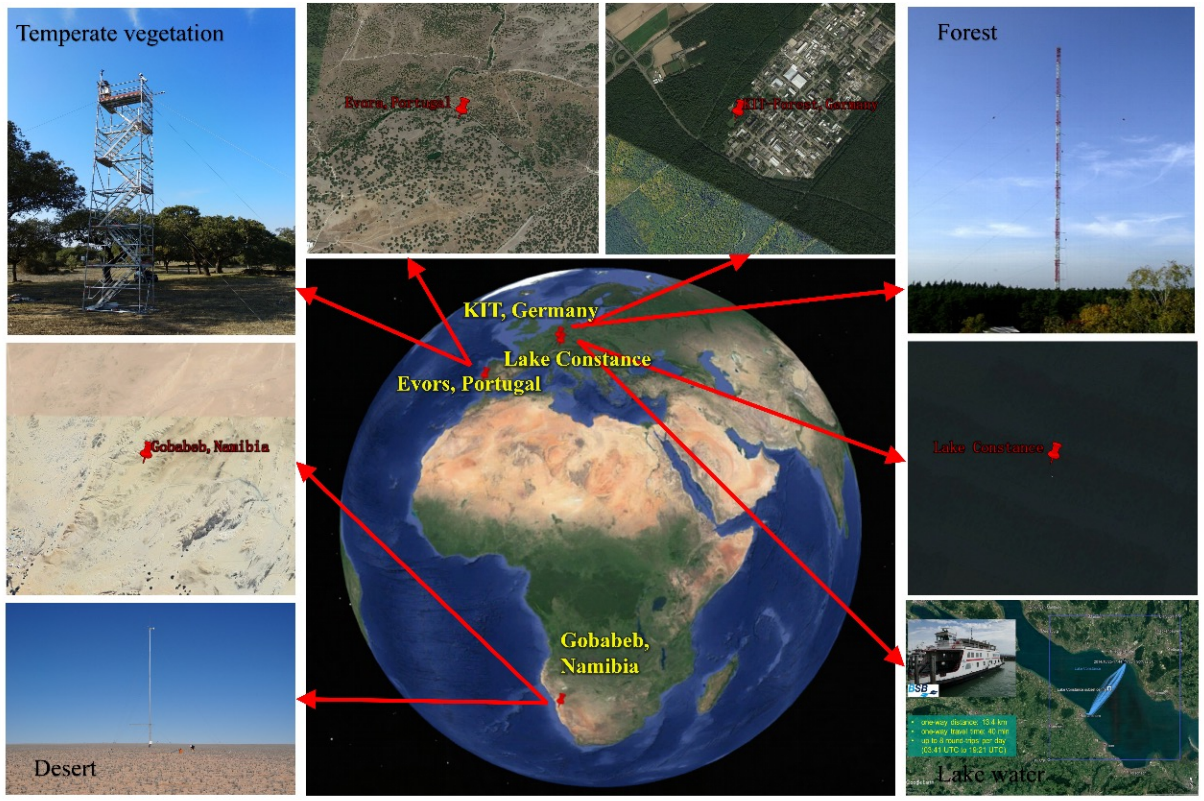

Location

Time series

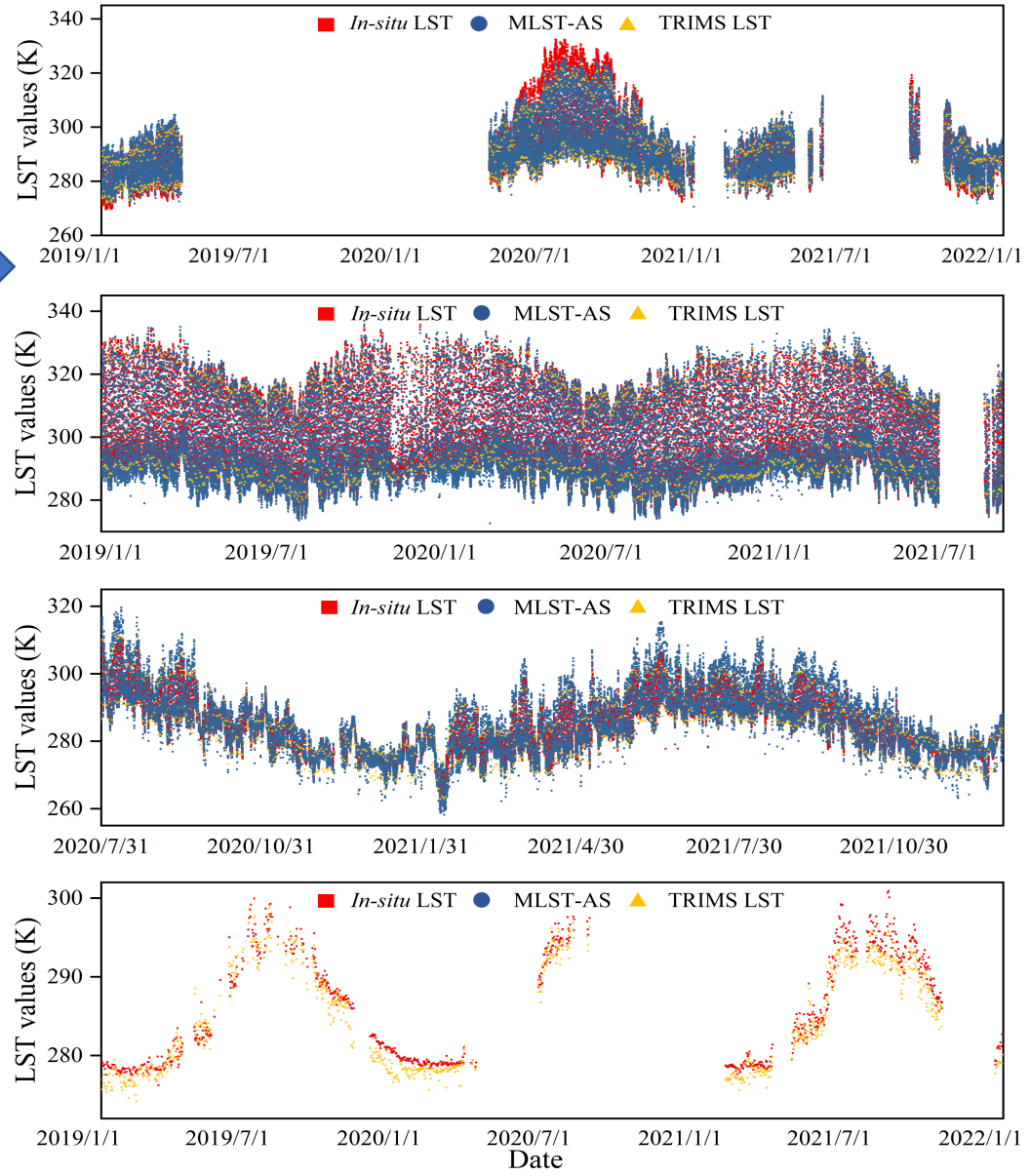

Investigation and Validation of TRIMS LST and MLST-AS

- Both all-weather LST products exhibit a high level of accuracy.
- The accuracy of MLST-AS is better than that of TRIMS LST across all land sites.
- MLST-AS and TRIMS LST exhibit better accuracy at the Gobabeb site and lower accuracy at Evora.

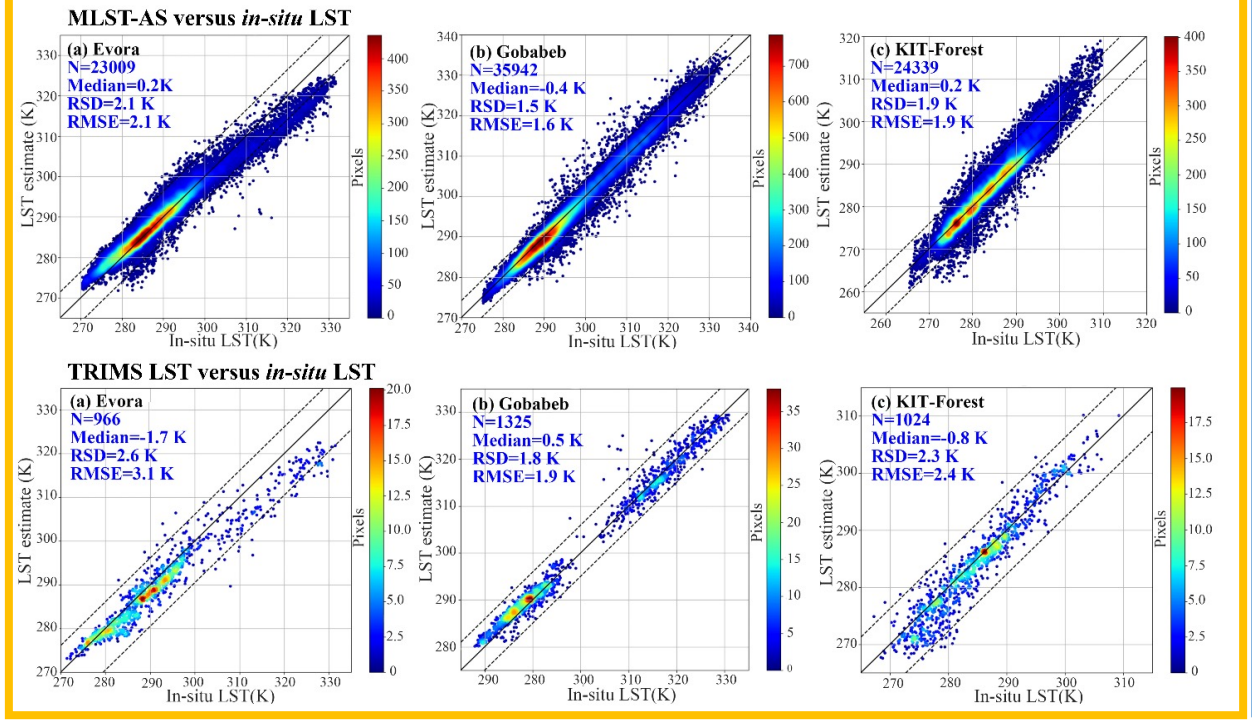

- Both MLST-AS and TRIMS LST demonstrate higher accuracy under clear-sky conditions .
- MLST-AS exhibits similar accuracy under different conditions at Evora and KIT-Forest, but displays significantly lower accuracy under unclear-sky conditions at Gobabeb.
- TRIMS LST exhibits the opposite pattern.

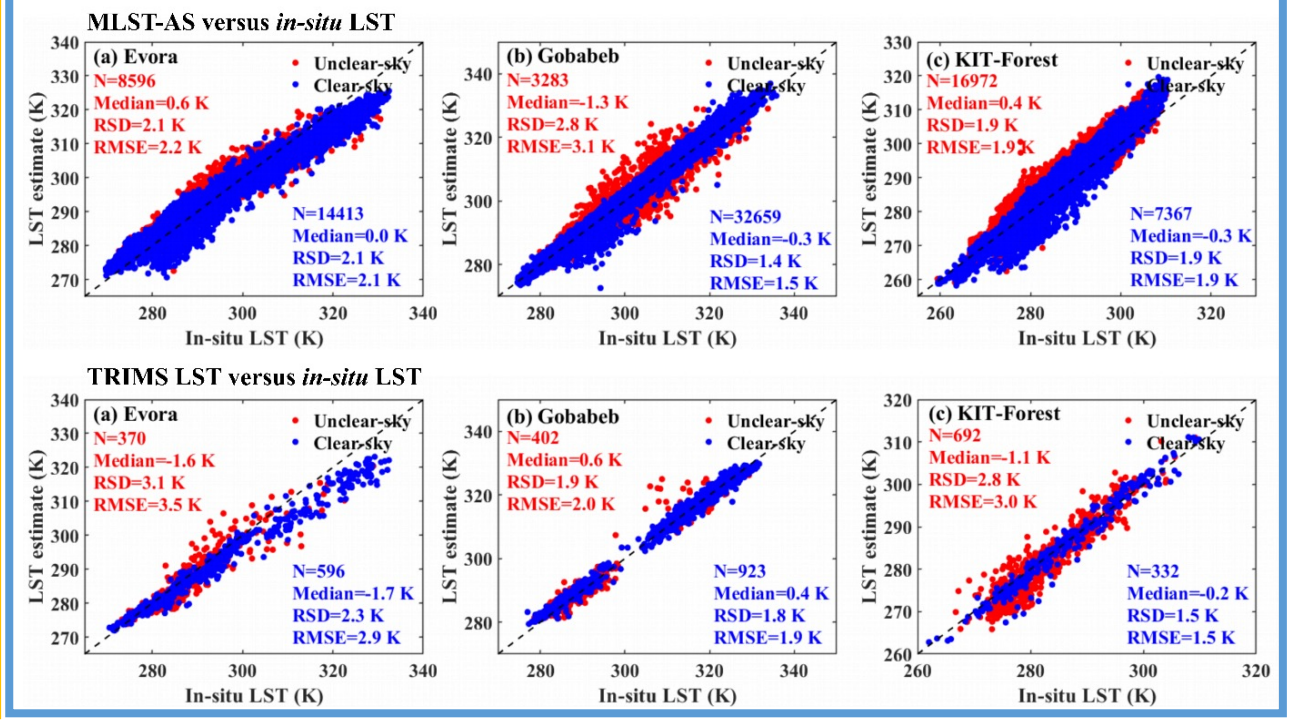

Investigation and Validation of TRIMS LST and MLST-AS

- The MLST-AS retrieval algorithm utilizes a land-water mask and generates LST values exclusively over land areas. Consequently, only the TRIMS LST values are validated against the obtained *in-situ* LWST measuremen at Lake Constance.
- TRIMS LST shows a similar accuracy to the land sites with a median value of -1.1 K and a RMSE of 1.6 K.
- A slightly higher accuracy for the TRIMS LST under clear-sky conditions compared to unclear-sky conditions.

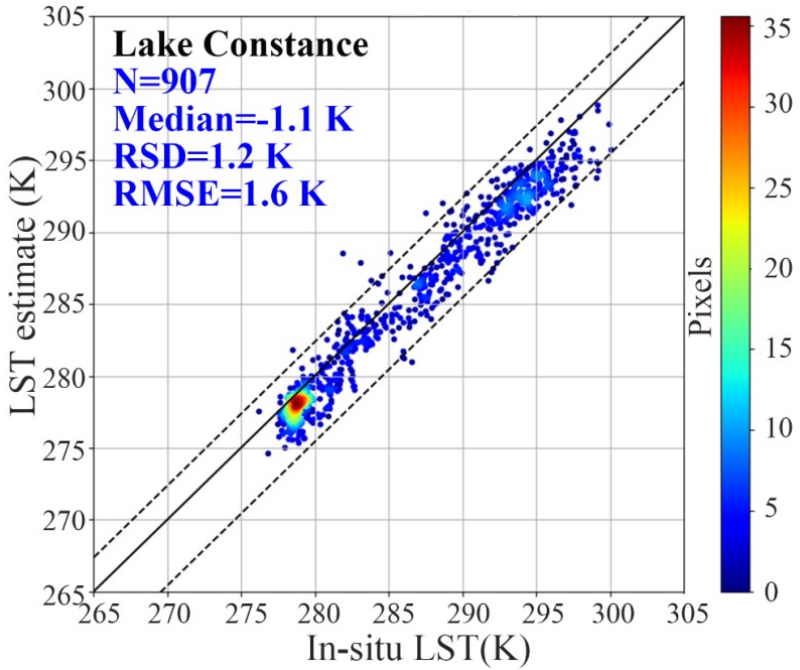

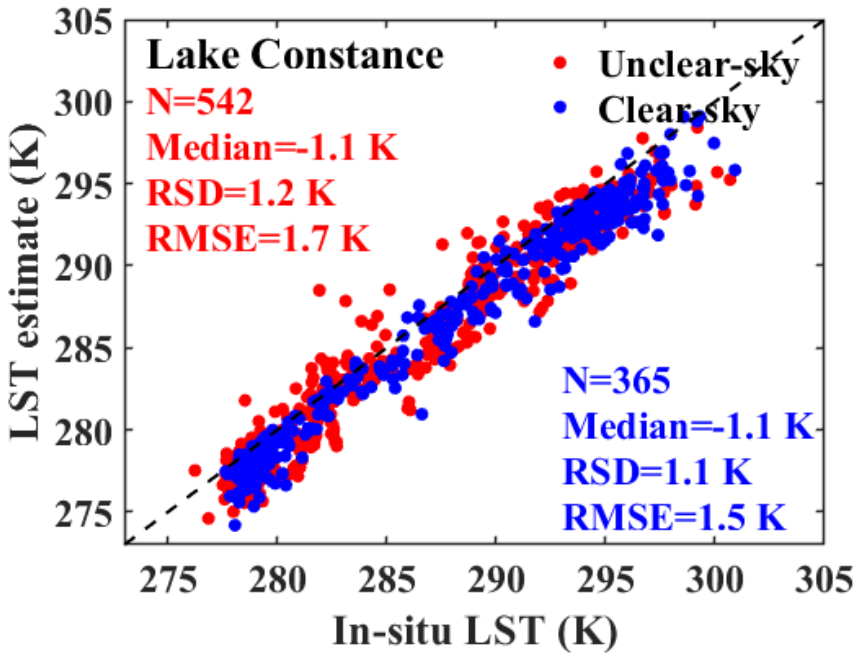

Actually, large water bodies present an ideal opportunity for validating satellite LST due to their homogeneity and isothermal characteristics. Therefore, there is a general anticipation that the validation accuracy for large water bodies (i.e., Lake Constance) would be better. For example, Yang et al. (2020) used different split-window algorithms (SWA) to perform LST retrieval based on Sentinel-3 SLSTR data, and the RMSEs over the Lake Constance site ranged from 0.49 K to 0.61 K.

Investigation and Validation of TRIMS LST and MLST-AS

- Due to the design of the underlying algorithms, under clear-sky conditions, the MLST-AS product is identical to the MLST product. Consequently, we exclusively compare TRIMS LST and its input MODIS LST with *in-situ* LST to quantify and analyze the uncertainty introduced by the TRIMS LST algorithm.
- TRIMS LST is an effective all-weather LST estimation method with similar accuracy to MODIS LST.
- TRIMS LST is heavily reliant on MODIS LST).
- The inapplicability of the retrieval algorithm of MODIS LST for estimating LWST extends to TRIMS LST, leading to low accuracy for TRIMS LST at Lake Constance.

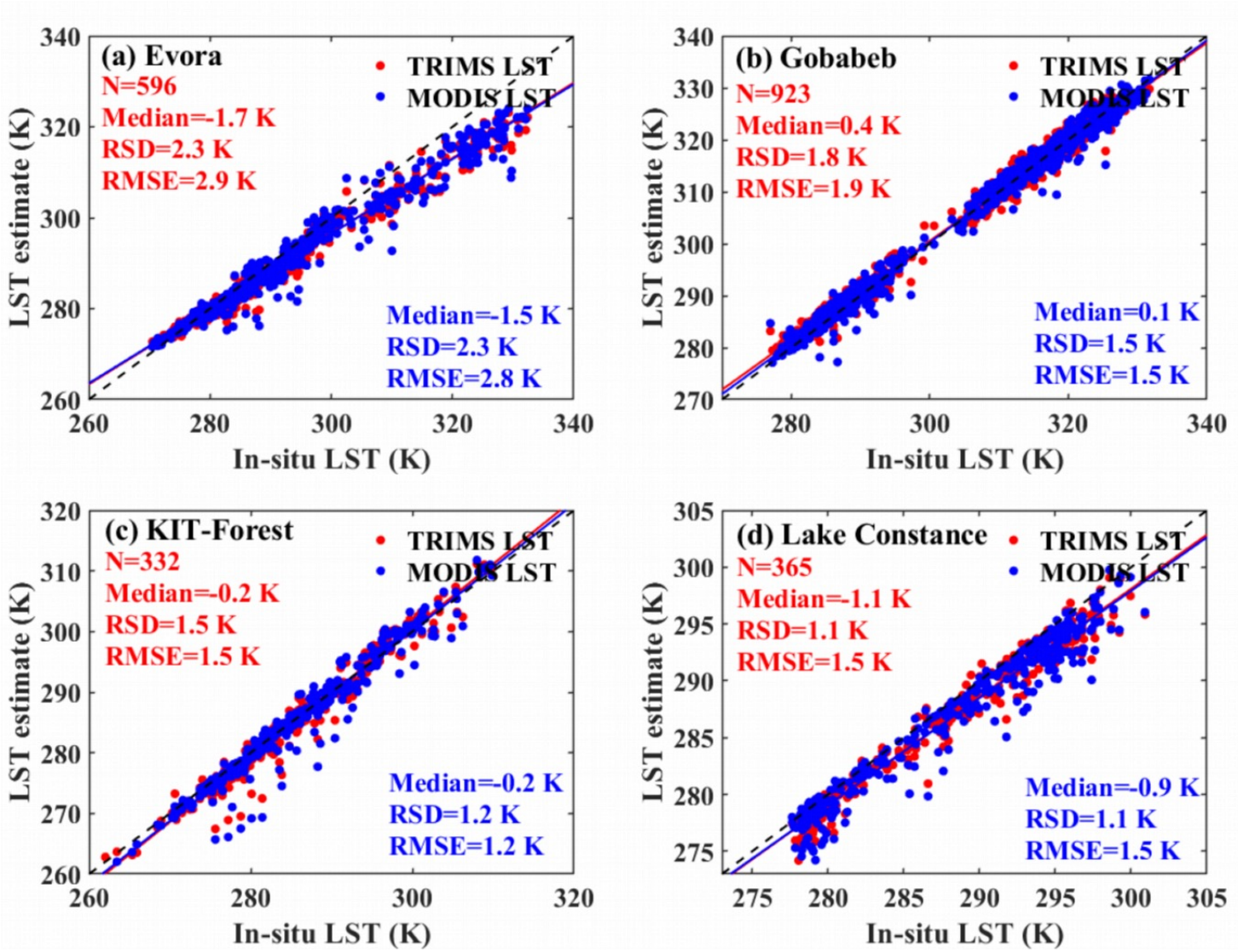

Outlook for the progress of Project 59318

I. ALL-WEATHER LST FROM UESTC, CHINA

II. LSA SAF (IPMA) ALL-SKY LST

III. VALIDATION AGAINST IN-SITU LST

IV. SPATIAL REPRESENTATION OF GROUND STATIONS IN LST VALIDATION

V. APPLICATION

SPATIAL REPRESENTATION

Objectives

- Validating the satellite retrieved LST
- How to consider the spatial representativeness of ground stations in LST validation?
- Quantify the uncertainty in the LST validation

EO and other data (2002-2012)

- Terra MODIS 6.0 level-3 LST Product (MOD11A1)
- ENVISAT AATSR Product (ENVISAT.ATS.LST_2P)
- 16 ground observations in China (Shown in Right)
- GLASS Broadband Emissivity from BNU
- Meteorological reanalysis data from CLDAS and GLDAS

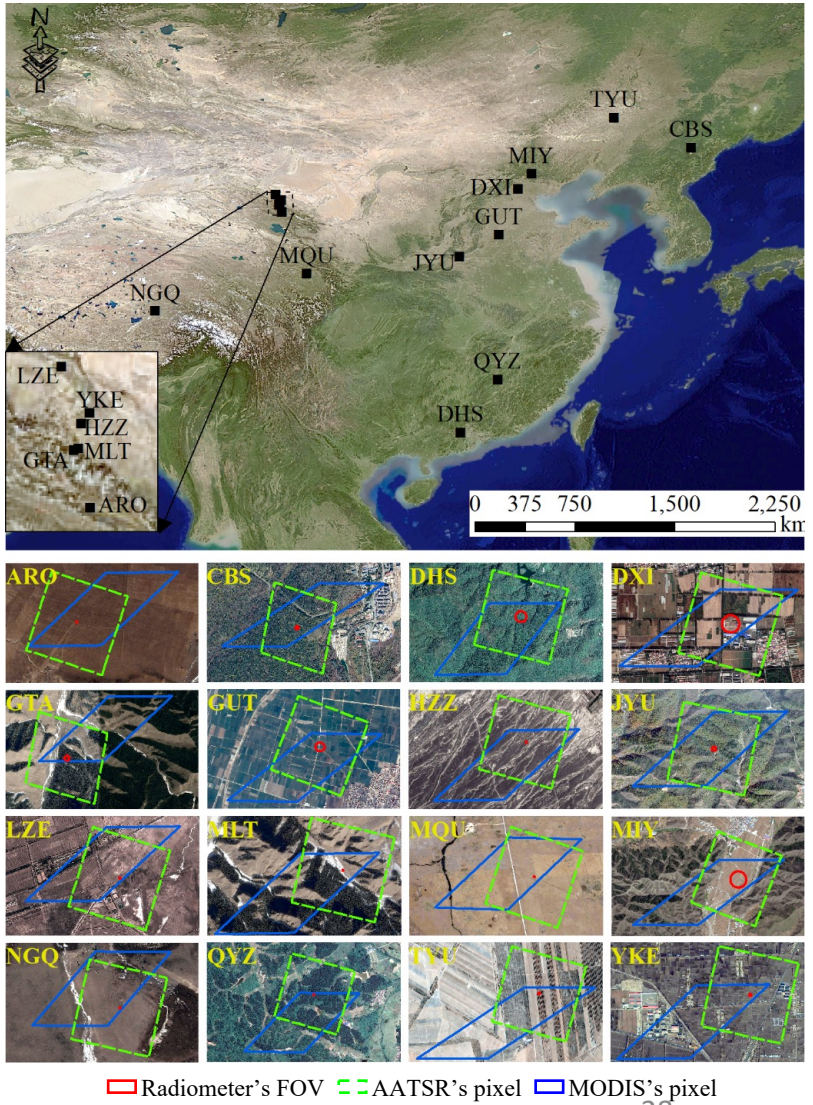

SPATIAL REPRESENTATION

Definition of Spatial Representativeness Indicator

$$SRI(t) = T_F(t) - T_P(t)$$

where *SRI* is the indicator for spatial representativeness; T_F and T_P are the true LST within the *in-situ* radiometer's FOV and satellite pixel, respectively, and simulated from Landsat LST.

Continuous, indicating the average state of temperature difference between the two scales

$$\begin{cases} T_F(t) = ATC_F(t) + \Delta DTC_F(t) + USC_F(t) \\ T_P(t) = ATC_P(t) + \Delta DTC_P(t) + USC_P(t) \end{cases}$$

Ignorable

Discrete, representing the temperature difference fluctuations of the two scales, affected by environmental factors, need to be continuous

$$SRI(t) = \Delta ATC(t) + \Delta DTC_{F-P}(t) + \Delta USC(t)$$

$$ATC(t) = \Delta \bar{T}_a + A \sin\left(\frac{2\pi t}{365} + \theta_0\right)$$

$$\Delta ATC(t) = ATC_F(t) - ATC_P(t)$$

Weather condition parameters, land surface parameters, etc.

$$\Delta USC(t) = g[x_1(t), x_2(t), \ldots \ldots x_n(t)]$$

Temporal variation model: $SRI_{TPR}(t) = \Delta \bar{T}_a + A \sin\left(\frac{2\pi t}{365} + \theta_0\right) + g[x_1(t), x_2(t), \ldots \ldots x_n(t)]$

SPATIAL REPRESENTATION

Validation

Conversion the *in-situ* LST to pixel scale associated with *SRI* as the bridge:

$$T_{P,in-situ}(t) = T_{in-situ}(t) - SRI_{TPR}(t)$$

❑ **Normal validation**

$$T_{SAT}(t) - T_{in-situ}(t) = \varepsilon_{\text{total,P-F}} = \varepsilon_{\text{SAT}}(t) + \varepsilon_{in-situ}(t) + \varepsilon_{\text{REP}}(t) + \varepsilon_{\text{time}}(t)$$

$$STD^2_{\text{total,P-F}} = STD^2_{\text{SAT}} + STD^2_{in-situ} + STD^2_{\text{REP}} + STD^2_{\text{time}}$$

❑ **Validation with spatial representativeness considered**

$$T_{SAT}(t) - T_{P,in-situ}(t) = \varepsilon_{\text{total,P-P}} = \varepsilon_{\text{SAT}}(t) + \varepsilon'_{\text{in-situ}}(t) + \varepsilon_{\text{time}}(t)$$

$$= \varepsilon_{\text{SAT}}(t) + \varepsilon_{in-situ}(t) + \varepsilon_{\text{SRI}}(t) + \varepsilon_{\text{time}}(t)$$

$$STD^2_{\text{total,P-P}} = STD^2_{\text{SAT}} + STD^2_{in-situ} + STD^2_{\text{SRI}} + STD^2_{\text{time}}$$

The accuracy of the satellite LST products/datasets

$$\text{MBE}_{SAT} = \frac{1}{N}\sum_{n=1}^{N}\left(\varepsilon_{\text{total,P-P}} - \varepsilon_{in-situ} - \varepsilon_{\text{SRI}} - \varepsilon_{\text{time}}\right)$$

$$STD^2_{\text{SAT}} = STD^2_{\text{total,P-P}} - STD^2_{in-situ} - STD^2_{\text{SRI}} - STD^2_{\text{time}}$$

The ground station's spatial representativeness influence in normal validation

$$\text{MBE}_{\text{REP}} = \frac{1}{N}\sum_{n=1}^{N}\left(\varepsilon_{\text{total,P-F}} - \varepsilon_{\text{total,P-P}} + \varepsilon_{\text{SRI}}\right)$$

$$STD^2_{\text{REP}} = STD^2_{\text{total,P-F}} - STD^2_{\text{total,P-P}} + STD^2_{\text{SRI}}$$

SPATIAL REPRESENTATION

Temporal-continuous *SRI*

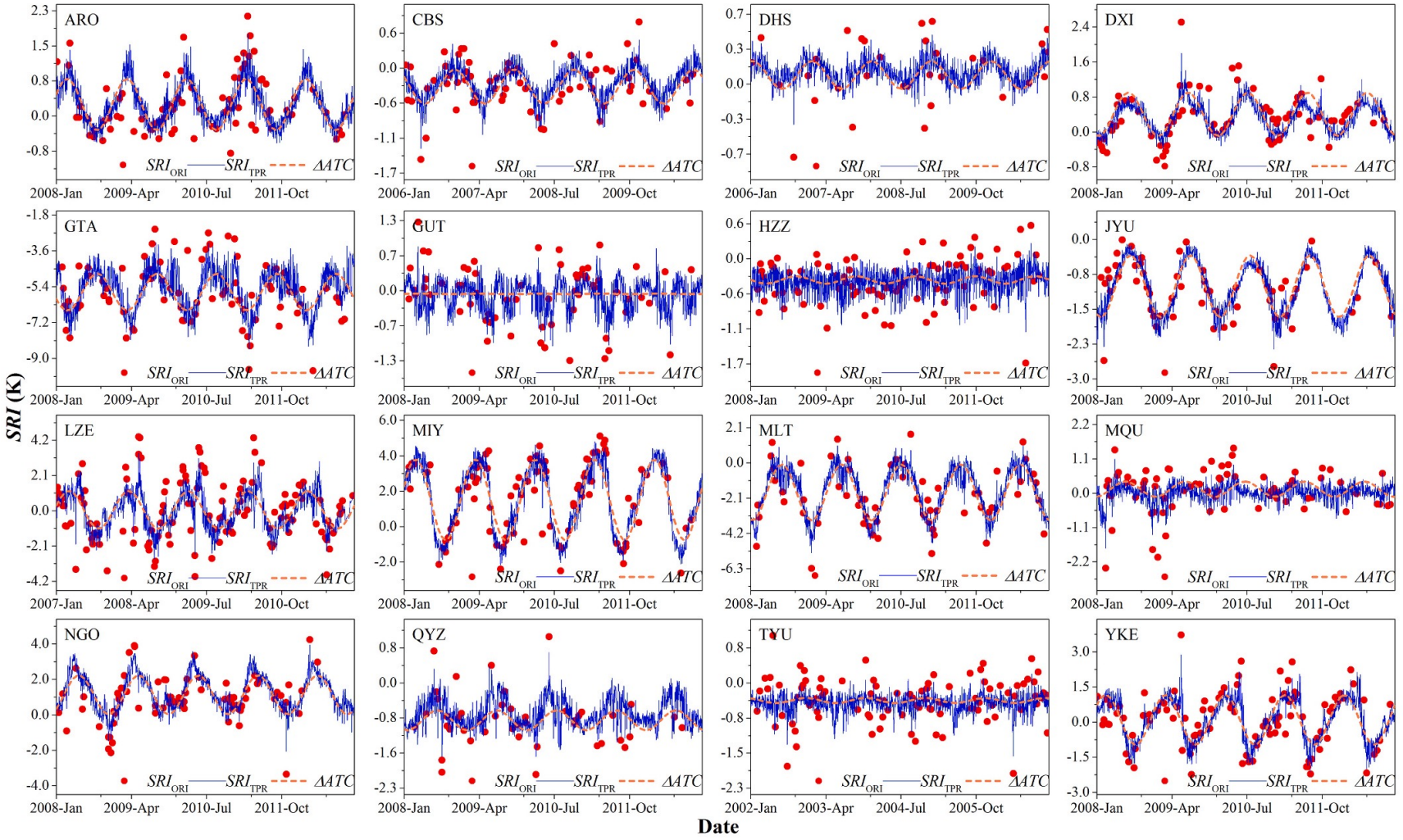

Fig. 2 *SRI* and Δ*ATC* for AATSR over the sixteen sites. The subscript ORI and TPR denote "original" and "temporal", respectively

- The temporal-continuous SRI shows the consistence with the original discrete SRI, it can catch the spatial representativeness variation in temporal.
- The spatial representativeness of a station depends on its underlying surface and weather conditions.

SPATIAL REPRESENTATION

Validation

Table 1. Validation of AATSR LST against T_{ground} and $T_{P,ground}$

Site		Sample size	$T_{SAT} - T_{ground}$			$T_{SAT} - T_{P,ground}$			Representativeness Error		Product Quality	
			μ_{total} (K)	σ_{total} (K)	R^2	μ_{total}' (K)	σ_{total}' (K)	R^2	e_{REP} (K)	μ_{REP} (K)	e_{SAT} (K)	μ_{SAT} (K)
ARO	D	63	0.62	3.26	0.95	0.99	3.13	0.95	−0.37	0.97	0.99	2.91
	N	89	1.98	1.85	0.97	–	–	–	–	–	–	–
CBS	D	9	1.78	1.71	0.84	1.50	1.64	0.86	0.31	0.84	1.48	1.25
	N	33	−0.58	2.06	0.98	–	–	–	–	–	–	–
DHS	D	7	2.08	1.27	0.96	2.15	1.29	0.96	−0.11	0.42	2.18	0.89
	N	13	0.16	0.45	0.99	–	–	–	–	–	–	–
DXI	D	29	3.00	1.72	0.98	3.59	1.93	0.98	−0.55	0.72	3.56	1.32
	N	108	−1.88	1.11	0.99	–	–	–	–	–	–	–
GTA	D	30	7.28	2.53	0.96	1.72	2.07	0.97	5.60	1.71	1.68	1.66
	N	84	−0.61	1.22	0.98	–	–	–	–	–	–	–
GUT	D	14	2.72	2.62	0.97	2.43	2.41	0.97	0.21	1.51	2.50	1.97
	N	41	−0.25	1.26	0.99	–	–	–	–	–	–	–
HZZ	D	92	2.51	1.79	0.99	2.16	1.82	0.99	0.37	0.07	2.14	1.56
	N	106	1.61	1.10	0.99	–	–	–	–	–	–	–
JYU	D	5	3.26	3.54	0.56	2.34	3.41	0.67	0.87	1.43	2.39	3.14
	N	29	−0.99	2.25	0.95	–	–	–	–	–	–	–
LZE	D	37	1.97	2.70	0.96	1.98	2.66	0.96	0.03	1.02	1.94	2.35
	N	47	2.62	1.67	0.98	–	–	–	–	–	–	–
MIY	D	54	2.42	2.14	0.97	4.40	2.04	0.98	−1.95	1.45	4.36	1.32
	N	84	1.32	1.85	0.99	–	–	–	–	–	–	–
MLT	D	12	−0.03	6.35	0.81	−1.63	5.25	0.82	1.67	3.72	−1.70	5.07
	N	29	4.54	1.57	0.96	–	–	–	–	–	–	–
MQU	D	16	1.93	2.33	0.94	2.07	2.28	0.94	−0.03	0.67	1.96	2.02
	N	11	3.05	1.99	0.96	–	–	–	–	–	–	–
NGQ	D	40	−3.57	2.47	0.94	−2.61	2.39	0.94	−0.94	0.95	−2.63	2.21
	N	64	1.67	1.41	0.98	–	–	–	–	–	–	–
QYZ	D	6	2.52	1.26	0.95	1.96	1.34	0.94	0.54	0.93	1.98	0.28
	N	17	−1.18	1.34	0.98	–	–	–	–	–	–	–
TYU	D	34	2.00	2.78	0.95	1.56	2.78	0.95	0.47	1.02	1.53	1.73
	N	36	−0.20	2.02	0.98	–	–	–	–	–	–	–
YKE	D	79	1.46	2.33	0.97	1.73	2.04	0.97	−0.27	1.27	1.73	1.77
	N	94	0.46	1.62	0.98	–	–	–	–	–	–	–
All	D	527	2.00	2.55	0.87	1.65	2.40	0.88	0.37	1.17	1.63	1.97
	N	885	0.73	1.55	0.98	–	–	–	–	–	–	–

Note: No scale conversion was performed at nighttime when LST is more spatially homogenous; D denotes daytime, N denotes nighttime.

- The AATSR LST shows a mean bias error and a standard deviation of error of 1.63 K and 1.97 K, respectively, when compared with in-situ LST.
- The spatial representativeness of ground station caused an systematic error of -1.95~5.6 K and random error of 0.07~3.72 K in normal validation against in-situ LST in the 16 selected stations.

SPATIAL REPRESENTATION

- **Defined the ground station's spatial representativeness and Temporal extended based on the temporal variation of LST.**
- **Quantified the temporal variation of spatial representativeness of 16 ground stations on MODIS and AATSR pixels by incorporating Landsat TM/ETM+ data and meteorological environmental parameters.**
- **Quantified the uncertainty in LST validation caused by ground station's spatial representativeness, shown that the station's spatial representativeness could cause a mean biases between – 1.95 K and 5.60 K and standard deviations between 0.07 K and 3.72 K on the normal validation results.**

Outlook for the progress of Project 59318

I. ALL-WEATHER LST FROM UESTC, CHINA

II. LSA SAF (IPMA) ALL-SKY LST

III. VALIDATION AGAINST IN-SITU LST

IV. SPATIAL REPRESENTATION OF GROUND STATIONS IN LST VALIDATION

V. APPLICATION

Applications

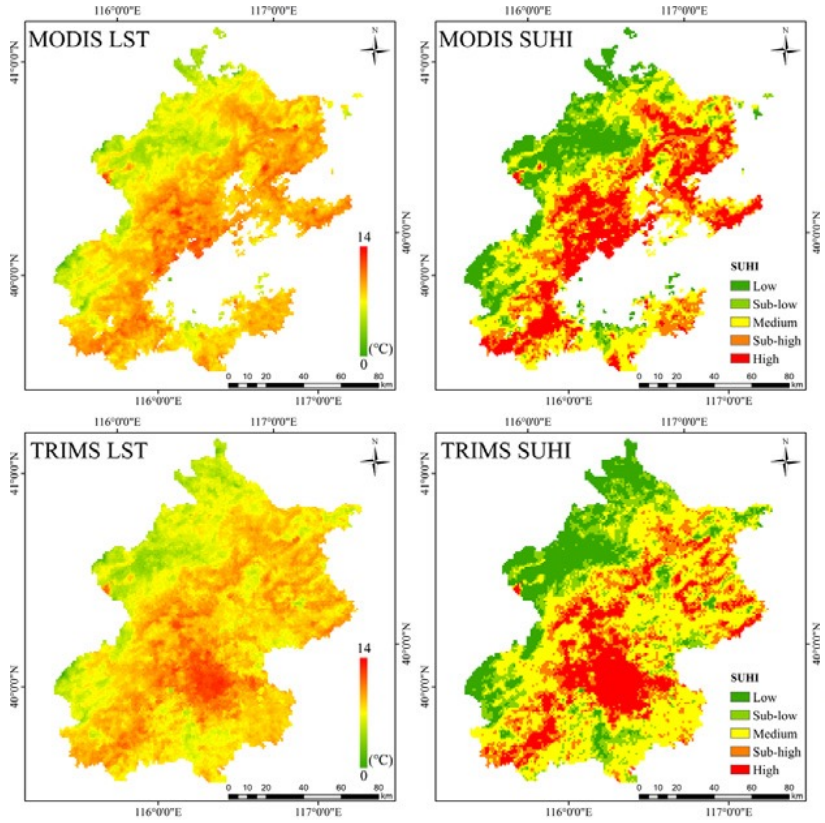

Spatial distribution of LST and SUHI at nighttime in Beijing on April 12

Urban-Heat-Island Monitoring
(Liao et al., 2022)

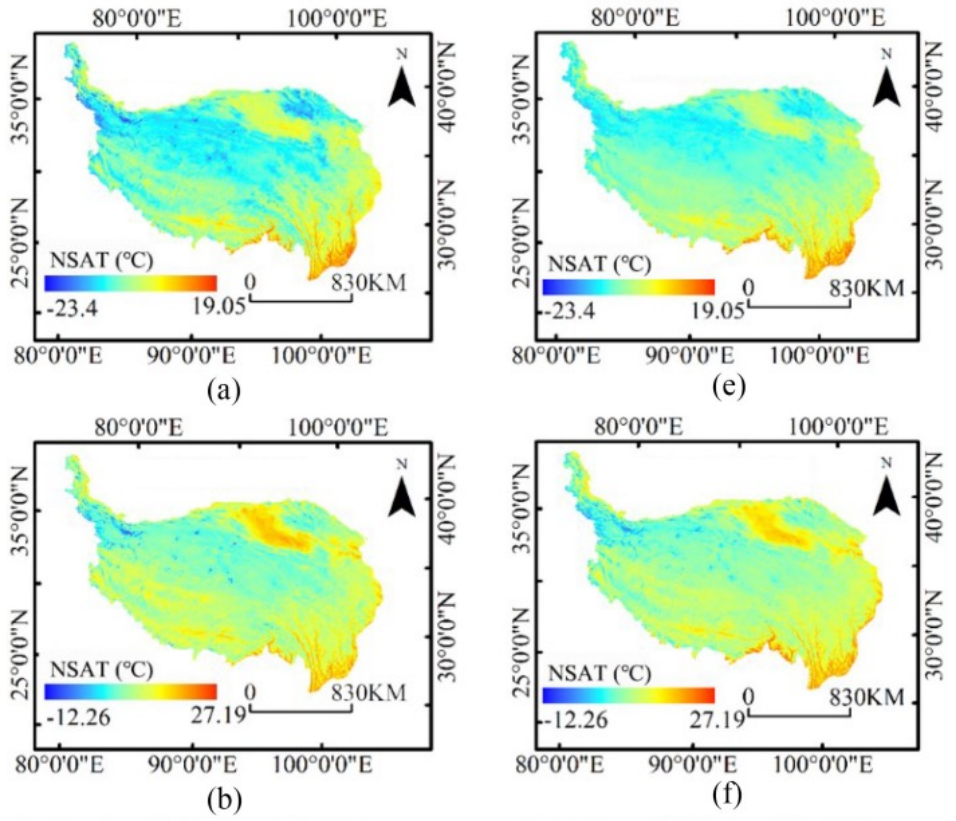

Near-surface T_a estimating
(Wang et al., 2022)

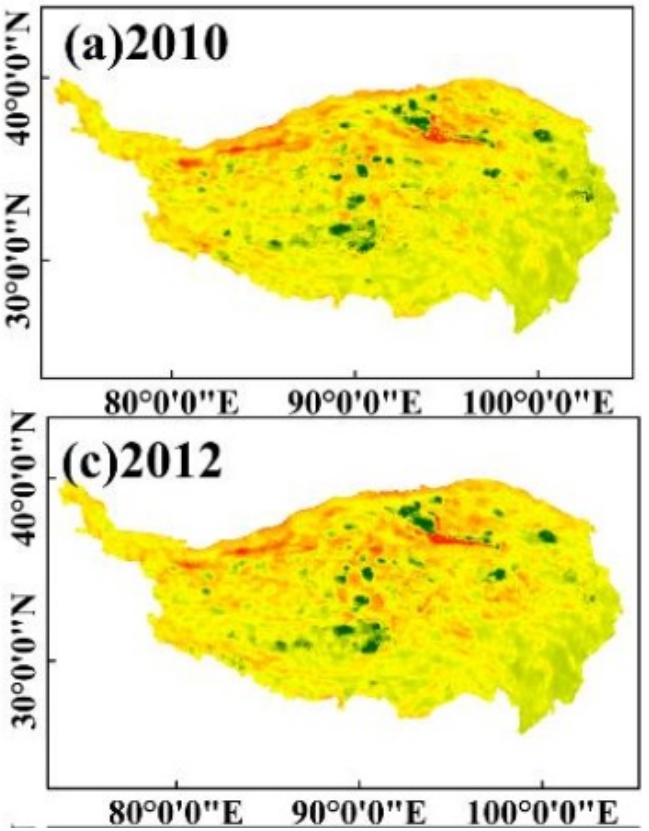

Near-surface T_a Lapse Rate
estimating (Zhong et al., 2023)

Summary and Outlook

Summary

- Updating the TRMIS LST in China and its surrounding areas
- Validated the two All-weather LST over Europe and Africa
- Proposed an method in quantifying the spatial representativeness of ground stations in LST validation
- Applied the TRIMS LST in UHI and Ta related subject

Outlook

- Extend the all-weather from current areas to global
- Further comprehensive validation combined the spatial representativeness of ground stations
- Explore more applications for the two All-weather LST

Publications

- **Algorithms:**

- Ding, L., Zhou, J., Li, Z.-L., Ma, J., Shi, C., Sun, S., Wang, Z., 2022. **Reconstruction of Hourly All-Weather Land Surface Temperature by Integrating Reanalysis Data and Thermal Infrared Data From Geostationary Satellites (RTG)**. *IEEE Trans. Geosci. Remote Sensing* 60, 1–17. https://doi.org/10.1109/TGRS.2022.3227074
- Tang, W., Xue, D., Long, Z., Zhang, X., Zhou, J., 2022. **Near-Real-Time Estimation of 1-km All-Weather Land Surface Temperature by Integrating Satellite Passive Microwave and Thermal Infrared Observations**. *IEEE Geosci. Remote Sensing Lett.* 19, 1–5.
- Wang, S., Zhou, J., Lei, T., Wu, H., Zhang, X., Ma, J., Zhong, H., 2020. **Estimating Land Surface Temperature from Satellite Passive Microwave Observations with the Traditional Neural Network, Deep Belief Network, and Convolutional Neural Network**. *Remote Sensing* 12, 2691.
- Zhang, X., Zhou, J., Liang, S., Chai, L., Wang, D., Liu, J., 2020. **Estimation of 1-km all-weather remotely sensed land surface temperature based on reconstructed spatial-seamless satellite passive microwave brightness temperature and thermal infrared data**. *ISPRS Journal of Photogrammetry and Remote Sensing* 167, 321–344.
- Zhang, X., Zhou, J., Liang, S., Wang, D., 2021. **A practical reanalysis data and thermal infrared remote sensing data merging (RTM) method for reconstruction of a 1-km all-weather land surface temperature**. *Remote Sensing of Environment* 260, 112437.

Publications

- **Validation and Application:**

- Meng, Y., Zhou, J., Göttsche, F.-M., Tang, W., Martins, J., Perez-Planells, L., Ma J., Wang, Z., 2023. **Investigation and validation of two all-weather land surface temperature products with in-situ measurements**. *Geo-spatial Information Science* (Accepted)
- Ma, J., Zhou, J., Liu, S., Göttsche, F.-M., Zhang, X., Wang, S., Li, M., 2021. **Continuous evaluation of the spatial representativeness of land surface temperature validation sites**. *Remote Sensing of Environment* 265, 112669.
- Liao, Y., Shen, X., Zhou, J., Ma, J., Zhang, X., Tang, W., Chen, Y., Ding, L., Wang, Z., 2022. **Surface urban heat island detected by all-weather satellite land surface temperature**. *Science of The Total Environment* 811, 151405.
- Wang, W., Zhou, J., Wen, X., Long, Z., Zhong, H., Ma, J., Ding, L., Qi, D., 2022. **All-Weather Near-Surface Air Temperature Estimation Based on Satellite Data Over the Tibetan Plateau**. *IEEE Journal of Selected Topics in Applied Earth Observations and Remote Sensing* 15, 1–1.
- Zhong, H., Zhou, J., Tang, W., Zhou, G., Wang, Z., Wang, W., Meng, Y., Ma, J., 2023. **Estimation of Near-Surface Air Temperature Lapse Rate Based on MODIS Data Over the Tibetan Plateau**. *IEEE Journal of Selected Topics in Applied Earth Observations and Remote Sensing* PP, 1–13.